

The First Structurally Characterized Metal (κ^2N,P)-Phosphinohydrazides: The Key to Understanding the Intramolecular Rearrangement $R_2P-NR'-NR'-M \rightarrow R'N=PR_2-NR'-M$. Metalloderivatives of Diisopropylphosphinohydrazines: Synthesis and Properties

Alexander N. Kornev,^{*,†} Natalia V. Belina,[†] Vyacheslav V. Sushev,[†] Georgy K. Fukin,[†] Evgenii V. Baranov,[†] Yuriy A. Kurskiy,[†] Andrei I. Poddelskii,[†] Gleb A. Abakumov,[†] Peter Lönnecke,[‡] and Evamarie Hey-Hawkins[‡]

[†]Razuvaev Institute of Organometallic Chemistry, Russian Academy of Sciences, 49 Tropinin Street, 603950 Nizhny Novgorod, Russia, and [‡]Institut für Anorganische Chemie, Universität Leipzig, Johannisallee 29, D-04103 Leipzig, Germany

Received January 23, 2009

A number of novel phosphinohydrazines, $iPr_2P-NPh-NPh-H$ (**1**), $iPr_2P-NH-NH-PiPr_2$ (**2**), $iPr_2P-NMe-NH-PiPr_2$ (**3**), and $H-NMe-NH-PiPr_2$ (**4**), were prepared and characterized. The interaction of **1** with 1 equiv of $n-BuLi$ afforded a complex compound $[Li(DME)_3][Li\{(NPh-NPh-PiPr_2)-\kappa^2M\}_2]$ (**5**). The reaction of **5** with $NiBr_2$ resulted in the formation of the first stable transition metal phosphinohydrazide $[Ni\{(NPh-NPh-PiPr_2)-\kappa^2N,P\}_2]$ (**6**). Similarly, the cobalt(II) derivative $[Co\{(NPh-NPh-PiPr_2)-\kappa^2N,P\}_2]$ (**7**) was prepared by the reaction of **1** with $Co[N(SiMe_3)_2]_2$. An X-ray study reveals formation of the complexes containing elongated N–N bonds (1.443(1), 1.466(2), and 1.470(2) Å for **5**, **6**, and **7**, respectively) as compared with the starting material **1** (1.407(1) Å). Nickel phosphinohydrazide **6** has a square-planar cis configuration; the cobalt complex **7** possesses a square-planar centrosymmetric trans configuration. The half-sandwich nickel(II) complex $[CpNi\{(NPh-NPh-PiPr_2)-\kappa^2N,P\}]$ (**8**) was prepared by prolonged heating of phosphinohydrazine **1** with $NiCp_2$ in toluene. The lithiation of **3** with $n-BuLi$ resulted in the formation of an iminophosphoranate $[LiN=P_iPr_2-NMe-P_iPr_2]$ (**13**) (in situ), which is the product of insertion of a P_iPr_2 group into the nitrogen–nitrogen bond. The hydrolysis of **13** followed by the addition of $CoCl_2$ gave the phosphino-iminophosphoranato complex $[CoCl_2\{(HN=P_iPr_2-NMe-P_iPr_2)-\kappa^2N,P\}]$ (**15**) according to X-ray investigation. The phosphinohydrazine **3** reacted with FeX_2 in toluene to form adducts (1:1) $[FeX_2\{(P_iPr_2-NMe-NH-P_iPr_2)-\kappa^2P,P'\}]$ ($X = Cl$ (**9**), Br (**10**)), while $CoCl_2$ gave the complex salt $[(Co(P_iPr_2-NMe-NH-P_iPr_2)-\kappa^2P,P')_2(\mu-Cl)_3][CoCl_3(THF)]$ (**11**). A THF solution of complex **11** shows thermochromic behavior.

Introduction

The intramolecular rearrangement of phosphinohydrazide to iminophosphoranate ligands which we reported earlier^{1–3} is a novel and useful approach to the synthesis of coordination and organometallic compounds. The rearrangements of mono-, bis-, and tris(diphenylphosphino)hydrazide ligands, $Ph_2P-NPh-NPh-$, $(Ph_2P)_2N-NPh-$,

and $(Ph_2P)_2N-N(PPh_2)-$, in the coordination sphere of nickel(II), cobalt(II), and iron(III) result in the formation of metal complexes of the phosphazene and phosphinoamide types depending on the starting ligand (Scheme 1).

Phosphinohydrazines (in contrast to the phosphinohydrazide ligands) are known to form stable complexes with transition metals.⁴ Their behavior does not differ from usual transition metal complexes with tertiary phosphines. The nitrogen atoms in these ligands have low basicity and, as a rule, do not take part in metal coordination.⁵ On the other hand, σ -N-bonded phosphinohydrazides of transition metals

*To whom correspondence should be addressed. Phone: +7 (831) 4627795. Fax: +7 (831) 4627497. E-mail: akornev@iomc.ras.ru.

(1) Fedotova, Y. V.; Kornev, A. N.; Sushev, V. V.; Kurskiy, Yu. A.; Mushtina, T. G.; Makarenko, N. P.; Fukin, G. K.; Abakumov, G. A.; Zakharov, L. N.; Rheingold, A. L. *J. Organomet. Chem.* **2004**, 689, 3060–3074.

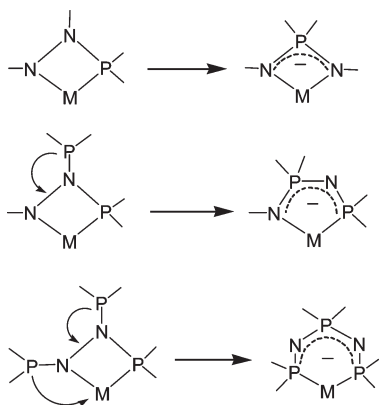
(2) Sushev, V. V.; Kornev, A. N.; Min'ko, Y. A.; Belina, N. V.; Kurskiy, Yu. A.; Kuznetsova, O. V.; Fukin, G. K.; Baranov, E. V.; Cherkasov, V. K.; Abakumov, G. A. *J. Organomet. Chem.* **2006**, 691, 879–889.

(3) Sushev, V. V.; Belina, N. V.; Fukin, G. K.; Kurskiy, Yu. A.; Kornev, A. N.; Abakumov, G. A. *Inorg. Chem.* **2008**, 47, 2608–2612.

(4) Appleby, T.; Woollins, J. D. *Coord. Chem. Rev.* **2002**, 235, 121–140.

(5) The exception is early and middle transition metal complexes with phosphino derivatives of 1,1-dialkylhydrazines, which demonstrate κ^2N,P -coordination: (a) Pavlik, S.; Jantscher, F.; Dazinger, G.; Mereiter, K.; Kirchner, K. *Eur. J. Inorg. Chem.* **2006**, 1006–1021. (b) Cowley, A. R.; Dilworth, J. R.; Nairn, A. K.; Robbie, A. J. *Dalton Trans.* **2005**, 680–693.

Scheme 1. Rearrangements of Mono-, Bis-, and Triphosphinohydrazides in Transition Metal Coordination Spheres ($M = \text{Fe}^{3+}$, Co^{2+} , Ni^{2+}).



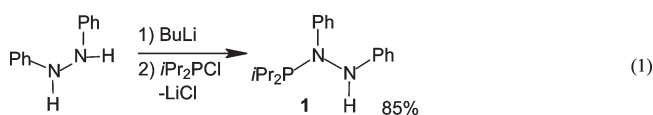
showing additional $\text{P} \rightarrow \text{M}$ coordination were not reported previously.⁶

The tendency of the phosphinohydrazide system toward rearrangement depends on several factors: (1) the energy of the $\text{N}-\text{N}$ bond, which strongly depends on the nature of the substituents on the nitrogen atoms; (2) the energy of the $\text{M}-\text{P}$ bond, which is determined by a combination of electronic effects of direct and back bonding between both atoms; and (3) the energy of the $\text{M}-\text{N}$ σ bond, which is usually weaker going from early to late transition metals. The mechanism of this rearrangement is still not clear; thus, further studies of transition metal phosphinohydrazides should help to answer this question.

Because a diisopropylphosphino group has better donor properties than a PPh_2 group, the corresponding metal phosphinohydrazides should be more stable toward intramolecular rearrangement. We have, therefore, prepared the novel diisopropylphosphinohydrazides $i\text{Pr}_2\text{P}-\text{NPh}-\text{NH}-\text{Ph}$ (**1**), $i\text{Pr}_2\text{P}-\text{NH}-\text{NH}-\text{P}i\text{Pr}_2$ (**2**), $i\text{Pr}_2\text{P}-\text{NMe}-\text{NH}-\text{P}i\text{Pr}_2$ (**3**), and $\text{H}-\text{NMe}-\text{NH}-\text{P}i\text{Pr}_2$ (**4**), and some of their alkali and transition metal complexes are reported below.

Results and Discussion

Synthesis of Diisopropylphosphinohydrazines. 1,2-Diphenyl-1-diisopropylphosphinohydrazine (**1**) was prepared by the reaction of the monolithium salt of 1,2-diphenylhydrazine with chlorodiisopropylphosphine in toluene (eq 1):

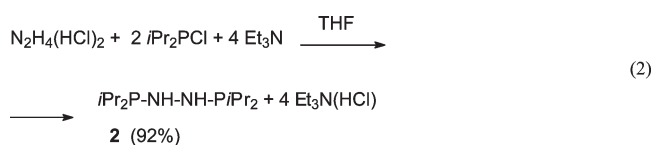


Phosphinohydrazine **1** is relatively air-stable and water-resistant. Stirring a toluene solution with an excess of water for an hour gave only 5% of $i\text{Pr}_2\text{P}(\text{O})\text{H}$, as shown by ^{31}P NMR monitoring. The ^1H NMR spectrum of **1** contains four groups of protons. The NH proton appears as a singlet resonance at 5.8 ppm, while the other groups (aromatic protons and methyl and methine

protons for the isopropyl group) reveal multiplets. The ^{31}P NMR spectrum of **1** exhibits a single resonance at δ 90.2 ppm.

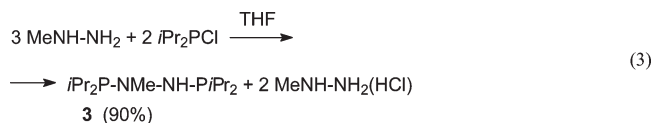
The structure of **1** was confirmed by X-ray analysis (see Supporting Information, Figure S1). Crystal data and some details of the data collection and refinement for **1** are given in Table 1; selected bond distances and angles are presented in Table 2. Each nitrogen atom in 1,2-diphenyl-1-diisopropylphosphinohydrazine has a slightly distorted trigonal-planar environment. The sum of the angles at $\text{N}(1)$ is 355.25° , smaller than the analogous value for the nitrogen atom in $\text{Ph}_2\text{P}-\text{NPh}-\text{NPh}-\text{H}$ (358.13°),¹ in accordance with better donor properties of the $\text{P}i\text{Pr}_2$ group. The $\text{P}-\text{N}$ and $\text{N}-\text{N}$ distances are 1.7312(9) and 1.407(1) Å, respectively, close to that in $\text{Ph}_2\text{P}-\text{NPh}-\text{NPh}-\text{H}$ (1.728(1) and 1.401(2) Å, respectively).¹

1,2-Bis(diisopropylphosphino)hydrazine, $i\text{Pr}_2\text{P}-\text{NH}-\text{NH}-\text{P}i\text{Pr}_2$ (**2**), was synthesized in another way, by the reaction of chlorodiisopropylphosphine with hydrazine dihydrochloride in the presence of an excess of triethylamine (eq 2).



Colorless crystals of **2** were obtained from toluene. The NH moiety could be identified by the presence of a doublet in the ^1H NMR spectrum at 3.36 ppm ($^2J_{\text{H,P}} = 8.3$ Hz). Isopropyl groups show two multiplets (1.52–1.78 and 0.9–1.30 ppm) assigned to the methine and methyl protons, respectively. The $^{31}\text{P}\{^1\text{H}\}$ NMR spectrum of **2** shows a single resonance at δ 73.6 ppm consistent with the equivalence of two $\text{P}i\text{Pr}_2$ groups. Note that the formation of tris(diisopropylphosphino)hydrazine does not take place even when an excess of $i\text{Pr}_2\text{P}(\text{Cl})$ is used.

1-Methyl-1,2-bis(diisopropylphosphino)hydrazine, $i\text{Pr}_2\text{P}-\text{NMe}-\text{NH}-\text{P}i\text{Pr}_2$ (**3**), was prepared by the interaction of methylhydrazine with chlorodiisopropylphosphine in a ratio of 3:2, without additional HCl abstractors (eq 3).



Compound **3** is an oily liquid (bp $100^\circ\text{C}/0.2$ mmHg). The ^1H NMR spectrum displays a singlet resonance at 2.78 ppm assignable to the methylamino group, a broad signal of the NH group at 3.37 ppm ($^2J_{\text{P,HN}}$ coupling is not resolved), two multiplets arising from nonequivalent methine protons of different $\text{P}i\text{Pr}_2$ groups, and two overlapping multiplets of $\text{C}(\text{CH}_3)_2$ groups. The $^{31}\text{P}\{^1\text{H}\}$ NMR spectrum of **3** contains two singlets at δ 88.9 and 66.5 ppm without visible coupling between the phosphorus nuclei. Cooling to 231 K causes a steadily broadening and disappearing of the signal at 88.9 ppm. We associate this observation with a rotational barrier about the $\text{P}-\text{N}$ bond in the fragment $i\text{Pr}_2\text{P}-\text{NMe}-$, which is obviously higher than in the $-\text{NH}-\text{P}i\text{Pr}_2$ group.

(6) The only example of a stable titanium phosphinohydrazide, $[(\text{C}_5\text{H}_5)_2\text{TiCl}_2(\text{Ph}_2\text{PNNMe}_2)-\kappa\text{N}]$, demonstrates no intramolecular $\text{P} \rightarrow \text{Ti}$ coordination (see ref 5).

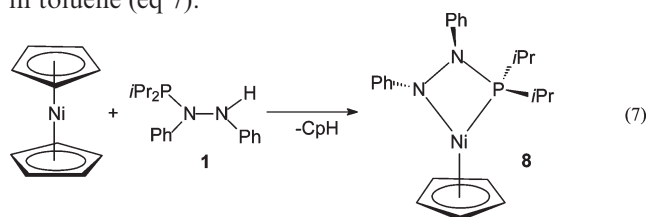
Table 1. Crystal and Structure Refinement

	1	5	6	7
empirical formula	C ₁₈ H ₂₅ N ₂ P	C _{58.50} H ₉₀ Li ₂ N ₄ O ₆ P ₂	C ₄₀ H ₅₆ N ₄ NiOP ₂	C ₃₆ H ₄₈ CoN ₄ P ₂
fw	300.37	1021.17	729.54	657.65
temp, K	100(2)	100(2)	100(2)	100(2) K
cryst system	monoclinic	monoclinic,	tetragonal	monoclinic
space group	<i>P2</i> ₁	<i>P2</i> ₁ / <i>c</i>	<i>P4</i> ₃ / <i>22</i>	<i>P2</i> ₁ / <i>c</i>
unit cell dimensions				
<i>a</i> , Å	8.5892(3)	16.8403(5)	9.4724(2)	8.5386(4)
<i>b</i> , Å	11.3094(4)	15.5848(5)	9.4724(2)	21.3880(9)
<i>c</i> , Å	9.0016(3)	23.5659(7)	41.780 (1)	9.5457(4)
α, deg	90	90	90	90
β, deg	101.894(1)	101.662(1)	90	102.904(1)
γ, deg	90	90	90	90
vol, Å ⁻³	855.63(5)	6057.3(3)	3748.8(2)	1699.2(1)
Z	2	4	4	2
density	1.166	1.120	1.293	1.285
(calculated), Mg/m ³				
abs coeff, mm ⁻¹	0.157	0.121	0.640	0.630
cryst size, mm ³	0.50 × 0.40 × 0.30	0.62 × 0.44 × 0.39	0.36 × 0.30 × 0.25	0.30 × 0.24 × 0.04
reflns collected	6444	53032	22642	9356
independent reflns	4414	12510	3690	2989
abs correction	[R(int) = 0.0096] semiempirical from equivalents, SADABS	[R(int) = 0.0292] semiempirical from equivalents, SADABS	[R(int) = 0.0250] semiempirical from equivalents, SADABS	[R(int) = 0.0173] semiempirical from equivalents, SADABS
max./min transmission	0.9544/0.9256	0.9545/0.9290	0.8564/0.8024	0.9752/0.8335
refinement method	full-matrix least-squares on <i>F</i> ²	full-matrix least- squares on <i>F</i> ²	full-matrix least- squares on <i>F</i> ²	full-matrix least- squares on <i>F</i> ²
data/restraints/params	4414/1/290	12510/64/1048	3690/0/330	2989/0/292
R indices [<i>I</i> > 2σ(<i>I</i>)]	R1 = 0.0262, wR2 = 0.0690	R1 = 0.0531, wR2 = 0.1412	R1 = 0.0279, wR2 = 0.0663	R1 = 0.0275, wR2 = 0.0753
R indices (all data)	R1 = 0.0264, wR2 = 0.0693	R1 = 0.0689, wR2 = 0.1519	R1 = 0.0292, wR2 = 0.0671	R1 = 0.0296, wR2 = 0.0765
largest diff. peak and hole, e Å ⁻³	0.274 and -0.152	0.822 and -0.836	0.334 and -0.179	0.428 and -0.168
	9	10	11	15
empirical formula	C ₁₃ H ₃₂ Cl ₂ FeN ₂ P ₂	C ₁₃ H ₃₂ Br ₂ FeN ₂ P ₂	C ₃₄ H ₈₀ Cl ₆ Co ₃ N ₄ O ₂ P ₄	C ₁₃ H ₃₂ Cl ₂ CoN ₂ P ₂
fw	405.10	494.02	1090.39	408.18
temp, K	130(2)	100(2)	130(2)	130(2)
cryst system	monoclinic	orthorhombic	monoclinic	monoclinic
space group	<i>P2</i> ₁ / <i>c</i>	<i>Pna2</i> ₁	<i>P2</i> ₁ / <i>n</i>	<i>P2</i> ₁ / <i>n</i>
unit cell dimensions				
<i>a</i> , Å	14.7925(1)	16.6898(5)	10.0820(1)	8.3283(1)
<i>b</i> , Å	11.0836(1)	10.9090(4)	27.9551(2)	16.0842(2)
<i>c</i> , Å	12.2774(1)	11.6196(4)	18.4152(3)	14.3787(2)
α, deg	90	90	90	90
β, deg	90.166(1)	90	103.442(1)	91.887(1)
γ, deg	90	90	90	90
vol, Å ⁻³	2012.92(3)	2115.6(1)	5048.0(1)	1925.04(4)
Z	4	4	4	4
density	1.337	1.551	1.435	1.408
(calculated), Mg/m ³				
abs coeff, mm ⁻¹	1.167	4.636	1.452	1.329
cryst size, mm ³	0.45 × 0.45 × 0.3	0.53 × 0.25 × 0.24	0.35 × 0.2 × 0.2	0.2 × 0.1 × 0.05
reflns collected	59935	13390	153679	47043
independent reflns	6139	4792	15410	5863
abs correction	[R(int) = 0.0228] semiempirical from equivalents, SCALE3 ABSPACK	[R(int) = 0.0216] semiempirical from equivalents, SADABS	[R(int) = 0.0798] semiempirical from equivalents, SCALE3 ABSPACK	[R(int) = 0.0444] semiempirical from equivalents, SCALE3 ABSPACK
max./min transmission	1/0.77722	0.4025/0.1925	1/0.83553	1/0.83289
refinement method	full-matrix least- squares on <i>F</i> ²	full-matrix least- squares on <i>F</i> ²	full-matrix least- squares on <i>F</i> ²	full-matrix least- squares on <i>F</i> ²
data/restraints/params	6139/0/309	4792/1/181	15410/0/532	5863/0/309
R indices [<i>I</i> > 2σ(<i>I</i>)]	R1 = 0.0210, wR2 = 0.0513	R1 = 0.0392, wR2 = 0.0959	R1 = 0.0406, wR2 = 0.0891	R1 = 0.0258, wR2 = 0.0535
R indices (all data)	R1 = 0.0277, wR2 = 0.0550	R1 = 0.0434, wR2 = 0.0980	R1 = 0.0887, wR2 = 0.1041	R1 = 0.0460, wR2 = 0.0581
largest diff. peak and hole, e Å ⁻³	0.531 and -0.287	2.250 and -0.423	1.441 and -0.662	0.697 and -0.267

Compound **7** was obtained as deep violet crystals in 85% yield. It has an anisotropic electron paramagnetic resonance (EPR) spectrum in the solid state with $g_{\parallel} = 2.656$, $g_{\perp} = 1.987$, and $g_{\text{iso}} = 2.268$ (see Supporting Information, Figure S2), which is indicative of a square-planar low-spin complex formation.⁸ The ether solution of **7** exhibits two absorptions at 420 and 538 nm in the UV–visible spectrum and no $^{31}\text{P}\{^1\text{H}\}$ NMR signal due to its paramagnetic nature. The IR spectrum of **7**, like that of compound **6**, contains strong absorption bands at 1230 and 1290 cm^{-1} assigned to the ν_{s} and ν_{as} P–N stretching vibrations.

Interestingly, the reaction of $[\text{Co}\{\text{N}(\text{SiMe}_3)_2\}_2]$ with 1,2-bis(diisopropylphosphino)hydrazine **2** is accompanied by nitrogen gas evolution and gave no isolable cobalt-containing products.

The mixed-ligand complex $[\text{CpNi}\{(\text{NPh}-\text{NPh}-\text{P}i\text{Pr}_2)-\kappa^2\text{N},\text{P}\}]$ (**8**) was prepared by prolonged heating of phosphinohydrazine **1** with biscyclopentadienylnickel in toluene (eq 7).



One of the cyclopentadienyl rings of $[\text{Cp}_2\text{Ni}]$ is substituted by a phosphinohydrazide ligand in the course of the reaction, as confirmed by a ^1H and ^{31}P NMR spectroscopy (δ_{P} 67.0 ppm). The UV/vis spectrum of **8** is similar to those of **6** and **7** and contains two absorption bands at 410 and 542 nm.

Single crystals of **6** and **7** were studied by X-ray crystallography. Compound **6** is a square-planar nickel(II) complex with a cis arrangement of the phosphino groups (Figure 2). The N–N bond in **6** (Table 3) is longer (1.466(2) Å) compared to that in the lithium salt **5** (1.443(1) Å) and that in **1** (1.407(1) Å), while the P–N bond is shorter (1.697(2) Å versus 1.727(1) Å in **5** and 1.7312(9) Å in **1**). These data indicate weakening of the N–N bond and strengthening of the P–N bond in the metallacycle. It is also worth noting that the nitrogen atoms of the phosphinohydrazide ligands have different geometries, which is dependent on the coordination mode of the ligand. The formation of the M–N–N–P cycle results in an appreciable deviation of the coordination sphere of the nitrogen atoms from planarity. A comparison of geometrical parameters of nitrogen atoms for compounds **1**, **5**, **6**, and **7** is given in Table 4.

Unlike in the nickel analog **6**, the phosphino groups in the cobalt phosphinohydrazide **7** occupy the trans positions, and the cobalt atom lies on a crystallographic inversion center (Supporting Information, Figure S3). The structural features of the metallacycle in **7** are close to those in **6**. The P–M bond in **7** is ca. 0.07 Å longer than

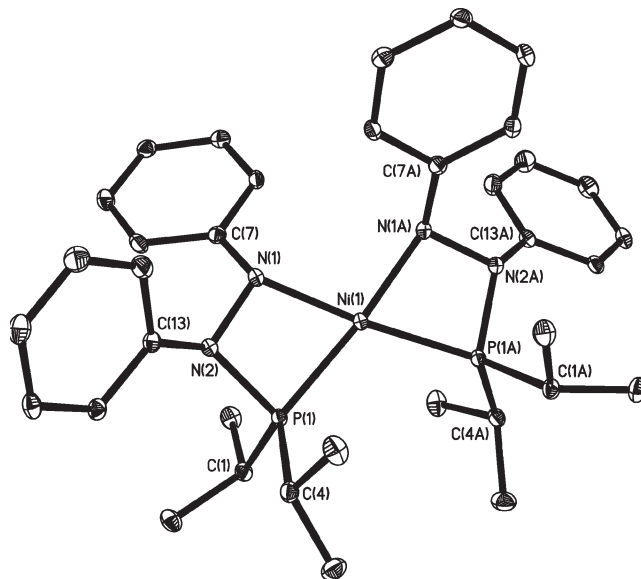


Figure 2. Molecular structure of $[\text{Ni}\{(\text{NPh}-\text{NPh}-\text{P}i\text{Pr}_2)-\kappa^2\text{N},\text{P}\}_2]$ (**6**). Hydrogen atoms are omitted for clarity. Ellipsoids are drawn at 30% probability.

Table 3. Selected Bond Lengths [Å] and Angles [deg] for $[\text{Ni}\{(\text{NPh}-\text{NPh}-\text{P}i\text{Pr}_2)-\kappa^2\text{N},\text{P}\}_2]$ (**6**) and $[\text{Co}\{(\text{NPh}-\text{NPh}-\text{P}i\text{Pr}_2)-\kappa^2\text{N},\text{P}\}_2]$ (**7**)

	6	7	
Ni(1)–N(1)	1.945(2)	Co(1)–N(1)	1.884(1)
Ni(1)–P(1)	2.1586(5)	Co(1)–P(1)	2.2285(4)
P(1)–N(2)	1.697(2)	P(1)–N(2)	1.715(1)
N(1)–N(2)	1.466(2)	N(1)–N(2)	1.470(2)
N(1A)–Ni(1)–N(1)	103.22(9)	N(1)–Co(1)–N(1A)	180.0
N(1)–Ni(1)–P(1A)	174.69(5)	N(1)–Co(1)–P(1)	71.36(4)
N(1)–Ni(1)–P(1)	71.52(5)	P(1)–Co(1)–P(1A)	180.0
P(1A)–Ni(1)–P(1)	113.75(3)	N(2)–P(1)–Co(1)	84.68(4)
N(2)–P(1)–Ni(1)	86.63(6)	N(2)–N(1)–Co(1)	105.53(8)
N(2)–N(1)–Ni(1)	101.9(1)	N(1)–N(2)–P(1)	98.34(8)
N(1)–N(2)–P(1)	98.7(1)		

in **6** (due to the trans influence of phosphino groups), while the N–M bond is ca. 0.06 Å shorter (Table 3). The P–N and N–N bond lengths in **6** and **7** are very similar. The main feature of the structures **6** and **7** is the elongated N–N bond. Considering how the transition metal phosphinohydrazides are prone to rearrangement (via insertion of a R_2P group into the N–N bond),^{1–3} it may be concluded that the first step of such a rearrangement is an elongation and splitting of this bond.

The N–N bond length in **6** and **7** is comparable to that of 1,2-diphenylhydrazides of thalium (1.471 Å)⁹ and lanthanum (1.471 Å),¹⁰ while derivatives of late transition metals are unknown.

Complexes of 1-Methyl-1,2-bis(diisopropylphosphino)hydrazine (3) with Transition Metal Halides. Attempts to prepare simple adducts of monophosphinohydrazines **1** and **4** with iron, cobalt, and nickel halides failed, perhaps owing to their being prone to dissociation in solution. On the other hand, the bidentate ligand 1-methyl-1,2-bis(diisopropylphosphino)hydrazine (**3**) was found to form stable adducts with FeCl_2 , FeBr_2 , and CoCl_2 . Heating of toluene or benzene solutions of **3** with FeCl_2 or FeBr_2 results in their fast dissolution. Slow cooling of the

(9) Katkova, M. A.; Fukin, G. K.; Fagin, A. A.; Bochkarev, M. N. *J. Organomet. Chem.* **2003**, 682, 218–223.

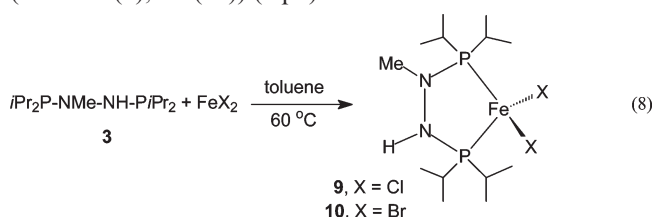
(10) Evans, W. J.; Lee, D. S.; Ziller, J. W.; Kaltsoyannis, N. *J. Am. Chem. Soc.* **2006**, 128, 14176–14184.

(8) It is notable that a solution of **7** in toluene has no EPR signal apparently due to the equilibrium between square-planar and high-spin tetrahedral configurations of **7** (which is typical for Co^{2+} complexes²). Oxygen addition to this solution leads to a new EPR spectrum, showing hyperfine coupling with a phosphorus atom (doublet, $A_{\text{P}} = 19.2$ G, $g_{\text{iso}} = 2.002$) and nitrogen atoms ($A_{\text{N}1} = 4.6$ G, $A_{\text{N}2} = 3.2$ G, $A_{\text{N}3} = 2.1$ G) that may be tentatively assigned to the formation of superoxide Co^{III} complex $[\text{Co}(\text{O}_2)\{(\text{NPh}-\text{NPh}-\text{P}i\text{Pr}_2)-\kappa^2\text{N},\text{P}\}\{(\text{NPh}-\text{NPh}-\text{P}i\text{Pr}_2)-\kappa\text{N}\}]$.

Table 4. The Sum of Bond Angles at Nitrogen Atoms in Compounds **1**, **5**, **6**, and **7**

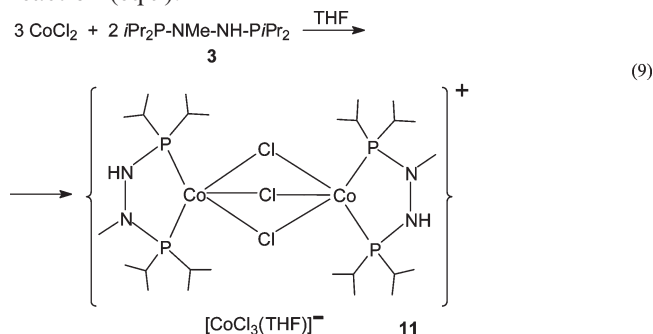
1	5	6	7
$\Sigma(\angle N_1) = 355.25$	$\Sigma(\angle N_1) = 353.33$	$\Sigma(\angle N_1) = 338.30$	$\Sigma(\angle N_1) = 341.27$
$\Sigma(\angle N_2) = 355.24$	$\Sigma(\angle N_2) = 359.71$	$\Sigma(\angle N_2) = 346.63$	$\Sigma(\angle N_2) = 342.87$

solutions to room temperature gave yellow crystals of the products $[\text{FeX}_2\{\text{P}(\text{iPr})_2\text{-NMe-NH-P}(\text{iPr})_2\}\text{-}\kappa^2\text{P,P}']$ ($\text{X} = \text{Cl}$ (**9**), Br (**10**)) (eq 8).



The IR spectra of **9** and **10** are similar, showing intense absorptions in the regions $3210\text{--}3240\text{ cm}^{-1}$ ($\nu(\text{NH})$) and $1100\text{--}1150\text{ cm}^{-1}$ ($\nu(\text{PN})$). The complexes are paramagnetic, showing no signal in the ^{31}P NMR spectrum. The molecular structure of **9** (Figure S4, Supporting Information) reveals the formation of a tetrahedral complex. The structural features of **9** (P–Fe and Fe–Cl bond lengths and the P–Fe–P angle; Table S1, Supporting Information) were found to be very close to those found in $[\text{FeCl}_2\{\text{P}(\text{iPr})_2\text{-CH}_2\text{-CH}_2\text{-P}(\text{iPr})_2\}\text{-}\kappa^2\text{P,P}']$.¹¹ The geometry of the nitrogen atoms in **9** is different: the sum of bond angles at N(1) is 357.54° (close to trigonal planar), while N(2) shows pyramidal geometry with a sum of bond angles of 339.28° . The molecular structure of **10** is very similar to that of complex **9**; however, these complexes are not isostructural. Examination of their chemical properties revealed the ability to absorb carbon monoxide at ambient conditions. However, no individual products were separated except for a case when **10** reacted with CO in the presence of a sodium amalgam.¹²

Unlike FeCl_2 , cobalt(II) chloride does not form a monomeric 1:1 compound; instead, the dark violet crystalline complex **11** was formed only in a 3:2 (metal/ligand) reaction (eq 9).



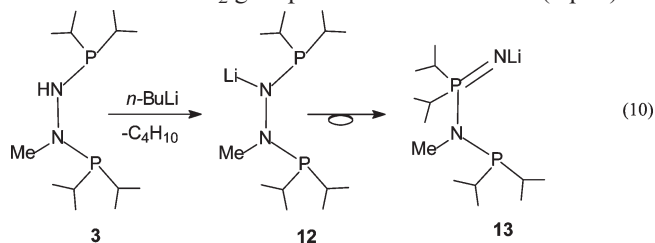
The IR spectrum of **11** is quite similar to that of **3**. It contains strong absorption bands at 3390 , 3216 cm^{-1}

($\nu(\text{NH})$), 1627 cm^{-1} ($\delta(\text{NH})$), and $1100\text{--}1200\text{ cm}^{-1}$ ($\nu(\text{PN})$ region). The IR spectrum also showed the presence of THF (1033 and 885 cm^{-1}).

The molecular structure of **11** (Figure 3, Table 5) consists of a Co-containing complex cation, complex anion, and a noncoordinated THF molecule. In the cationic part of the molecule, two $\text{Co}(\text{P}(\text{iPr})_2\text{-NMe-NH-P}(\text{iPr})_2)$ moieties are linked by three bridging chloro ligands. Two Co–Cl bonds (at each cobalt atom) are short ($2.3077(7)\text{--}2.340(7)\text{ \AA}$), and one is longer ($2.4546(7)$ and $2.4863(7)\text{ \AA}$), so that each cobalt atom lies in the center of a distorted tetragonal pyramid in which the chlorine atoms occupy two equatorial and the apical position. The third cobalt ion in the $[\text{CoCl}_3(\text{THF})]^-$ anion is tetrahedrally coordinated. The structural features of the $\text{P}_2\text{N}_2\text{Co}$ metallacycle in **11** are very similar to those found in **9**. The Co–P bond lengths ($2.1540(8)\text{--}2.2003(7)\text{ \AA}$) are noticeably smaller than the Fe–P one ($2.4571(3)$ and $2.4511(3)\text{ \AA}$), while internal P–Co–P bond angles ($85.22(3)^\circ$ and $84.37(3)^\circ$) in **11** are slightly bigger than the P–Fe–P angle ($82.06(1)^\circ$) in **9**.

Solutions of **11** in THF demonstrate a thermochromic behavior. Increasing the temperature of the THF solution from 4 to 60°C results in an increase of the intensity of the absorptions at 510 and 382 nm (Figure S5, Supporting Information), which corresponds to a steady change in color from dark cherry to greenish-blue, respectively. This phenomenon may be explained by a dissociation equilibrium of the complex cation in THF solution. Compound **11** does not change its thermochromic properties after prolonged heating (4 weeks) at 60°C . Dark cherry solutions of **11** in CH_2Cl_2 (noncoordinated solvent) do not exhibit thermochromic behavior.

The 1-Methyl-1,2-bis(diisopropylphosphino)hydrazide Ligand and Its Rearrangement. We attempted to synthesize cobalt(II) 1-methyl-1,2-bis(diisopropylphosphino)hydrazide by the reaction of **3** (2 equiv) with $[\text{Co}\{\text{N}(\text{SiMe}_3)_2\}_2]$ in toluene. However, no individual products could be separated from the deep brown reaction mixture. In another approach, we tried to use the reaction between CoCl_2 and lithiated **3**. A detailed investigation has shown that the lithiated **3** (which was prepared in situ by the reaction of **3** with butyl lithium) is not stable and rearranges to its isomer **13**, which is the product of insertion of a $\text{P}(\text{iPr})_2$ group into the N–N bond (eq 10):



(11) Hermes, A. R.; Girolami, G. S. *Inorg. Chem.* **1988**, *27*, 1775–1781.

(12) Carbonylation of **10** in the presence of a stoichiometric amount of sodium amalgam afforded a diamagnetic product $[\text{Fe}(\text{CO})_3\{\text{P}(\text{iPr})_2\text{-NMe-NH-P}(\text{iPr})_2\}\text{-}\kappa^2\text{P,P}']$ (see the Supporting Information), which exhibits two doublets in the $^{31}\text{P}\{\text{H}\}$ NMR spectrum at 187.6 and 167.3 ppm ($J_{\text{P,P}} = 63\text{ Hz}$).

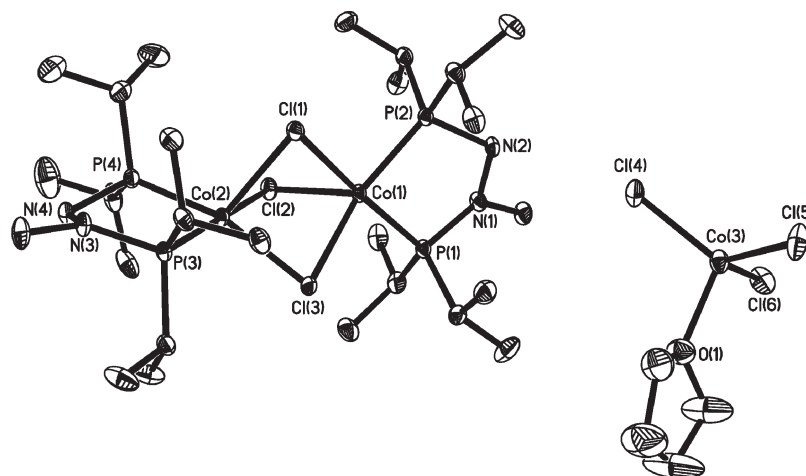
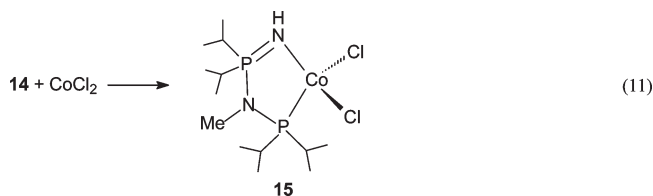


Figure 3. Molecular structure of $[\text{Co}\{(\text{PiPr}_2\text{-NMe-NH-PiPr}_2)\text{-}\kappa^2\text{P,P}'\}_2(\mu\text{-Cl})_3][\text{CoCl}_3(\text{THF})]$ (**11**). Hydrogen atoms are omitted for clarity. Ellipsoids are drawn at 30% probability.

Table 5. Selected Bond Lengths [Å] and Angles [deg] for $[\text{Co}\{(\text{PiPr}_2\text{-NMe-NH-PiPr}_2)\text{-}\kappa^2\text{P,P}'\}_2(\mu\text{-Cl})_3][\text{CoCl}_3(\text{THF})]$ (**11**)

Co(1)–Co(2)	2.9351(4)	P(2)–Co(1)–P(1)	85.22(3)
Co(1)–P(2)	2.1723(7)	P(4)–Co(2)–P(3)	84.37(3)
Co(1)–P(1)	2.1915(7)	P(2)–Co(1)–Cl(1)	92.64(3)
Co(2)–P(4)	2.1540(8)	P(1)–Co(1)–Cl(1)	173.76(3)
Co(2)–P(3)	2.2003(7)	P(2)–Co(1)–Cl(3)	161.54(3)
Co(1)–Cl(1)	2.3077(7)	P(1)–Co(1)–Cl(3)	92.35(3)
Co(1)–Cl(2)	2.4546(7)	Cl(1)–Co(1)–Cl(3)	87.83(2)
Co(2)–Cl(1)	2.4863(7)	P(2)–Co(1)–Cl(2)	113.93(3)
Co(2)–Cl(2)	2.3066(7)	P(1)–Co(1)–Cl(2)	101.67(3)
P(1)–N(1)	1.682(2)	Cl(1)–Co(1)–Cl(2)	84.56(2)
P(2)–N(2)	1.707(2)	Cl(3)–Co(1)–Cl(2)	84.50(2)
P(3)–N(3)	1.688(2)	N(1)–P(1)–Co(1)	107.34(8)
P(4)–N(4)	1.703(2)	N(2)–P(2)–Co(1)	109.76(9)
N(1)–N(2)	1.426(3)	N(2)–N(1)–P(1)	117.6(2)
N(3)–N(4)	1.434(3)	N(1)–N(2)–P(2)	110.3(2)

The $^{31}\text{P}\{^1\text{H}\}$ NMR monitoring of the reaction mixture revealed no signal at room temperature, apparently due to dynamic behavior in solution. Cooling the reaction mixture to -45°C also showed no changes in the $^{31}\text{P}\{^1\text{H}\}$ NMR spectrum. Stoichiometric hydrolysis of the reaction mixture (1:1) gave a product which exhibits a doublet in the $^{31}\text{P}\{^1\text{H}\}$ NMR spectrum at 68.0 and 59.9 ppm ($J_{\text{P,P}} = 41$ Hz). We assumed that this product is the iminophosphorane $i\text{Pr}_2\text{P-NMe-PiPr}_2\text{=NH}$ (**14**). The confirmation of the proposed rearrangement was found in the reaction of **14** with cobalt(II) chloride in an equimolar ratio, which results in the formation of a blue crystalline precipitate **15** (eq 11).



The IR spectrum of **15** shows broad and strong absorptions in the region $1000\text{--}1200\text{ cm}^{-1}$, which is indicative of the presence of a $\text{N-P}^{\text{V}}=\text{N}$ fragment in the molecule. The X-ray structure analysis revealed the formation of the cobalt(II) chloride phosphazene complex **15** (Figure 4, Table 6).

Complex **15** contains three different P–N bonds, one of which (short P(1)–N(1), 1.594(1) Å) has double-bond

character; the others (P(1)–N(2), 1.674(1); N(2)–P(2), 1.712(1) Å) are P–N single bonds. When compounds **15** and **7** are compared, it can be noted that the Co(1)–P(2) bond length (2.3506(4) Å) in the five-membered ring is larger than the Co(1)–P(1) one (2.2285(4) Å) in the four-membered ring in **7**. This may indicate stronger interaction of the cobalt and phosphorus in **7**. In **15**, both nitrogen atoms in the almost planar metallacycle have a planar environment, in contrast to that found in **7**.

When discussing the stability and chemical behavior of lithium salts of phosphinohydrazides, we should note that these properties depend largely on the structure of the compound and the nature of the substituents at the nitrogen and phosphorus atoms. Thus, lithium derivatives of 1,1-diphenylphosphino-2-*tert*-butylhydrazine, $\text{LiN}t\text{Bu-N}(\text{PPh}_2)_2$, and tris(diphenylphosphino)hydrazine, $\text{LiN}(\text{PPh}_2)\text{-N}(\text{PPh}_2)_2$,³ are not stable and decompose during preparation. In our opinion, the critical factor influencing the stability of the compounds is the strength of the nitrogen–nitrogen bond. A negative charge at a nitrogen atom in lithium phosphinohydrazides causes weakening and elongation of the N–N bond. Therefore, the rearrangement of the lithium bisphosphinohydrazide **12** was not unexpected. It is worth noting that this rearrangement proceeds in good yield, almost quantitatively.

Conclusions

The present work highlights the behavior of metal phosphinohydrazides of different types. A negative charge at the hydrazido nitrogen promotes the rearrangement of phosphinohydrazide to iminophosphoranate. So, lithium bisphosphinohydrazide, $i\text{Pr}_2\text{P-NMe-NLi-PiPr}_2$ (**12**), was found to rearrange quantitatively in THF solution to iminophosphoranate $\text{LiN}=\text{PiPr}_2\text{-NMe-PiPr}_2$ (**13**).

The complex salt $[\text{Li}(\text{DME})_3][\text{Li}\{(\text{NPh-NPh-PiPr}_2)\text{-}\kappa\text{N}\}_2]$ (**5**), being stable at room temperature, has an elongated N–N bond compared to that of the starting compound, HNPh-NPh-PiPr_2 . Herein, we have successfully synthesized the first examples of stable transition metal phosphinohydrazides with $\kappa^2\text{N,P}$ coordination, $[\text{M}\{(\text{NPh-NPh-PiPr}_2)\text{-}\kappa^2\text{N,P}\}_2]$ (M = Ni (**6**), Co (**7**)). These compounds demonstrate noticeably longer N–N bond distances compared with those

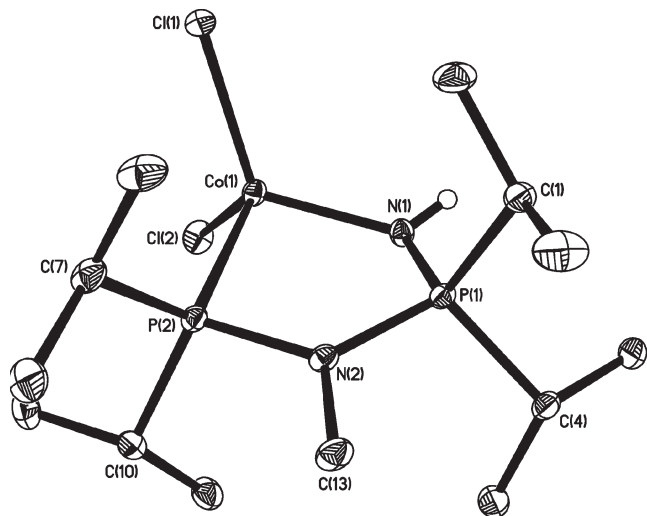


Figure 4. Molecular structure of $[\text{CoCl}_2\{(\text{HN}=\text{P}i\text{Pr}_2-\text{NMe}-\text{P}i\text{Pr}_2)-\kappa^2\text{N,P}\}]$ (**15**). Hydrogen atoms other than H1n are omitted for clarity. Ellipsoids are drawn at 30% probability.

Table 6. Selected Bond Lengths [Å] and Angles [deg] for $[\text{CoCl}_2\{(\text{HN}=\text{P}i\text{Pr}_2-\text{NMe}-\text{P}i\text{Pr}_2)-\kappa^2\text{N,P}\}]$ (**15**)

Co(1)–N(1)	1.950(1)	N(1)–Co(1)–P(2)	87.62(4)
Co(1)–Cl(1)	2.2570(4)	N(1)–P(1)–N(2)	105.89(6)
Co(1)–P(2)	2.3506(4)	N(2)–P(2)–Co(1)	100.57(4)
P(1)–N(1)	1.594(1)	P(1)–N(1)–Co(1)	122.46(7)
P(1)–N(2)	1.674(1)	P(1)–N(1)–H(1N)	108.1(15)
P(2)–N(2)	1.712(1)	Co(1)–N(1)–H(1N)	121.7(15)
N(1)–H(1N)	0.75(2)	P(1)–N(2)–P(2)	120.31(7)

of lithium salt **5** that may be also imposed by the ring strain of the four-membered metallacycle. So, we consider weakening and elongation of the N–N bond as a first step of the rearrangement. 1,2-Bisdiisopropylphosphino-methylhydrazine, $i\text{Pr}_2\text{P}-\text{NMe}-\text{NH}-\text{P}i\text{Pr}_2$ (**3**), forms stable complexes with iron(II) and cobalt(II) halides. The complex salt $\{[\text{Co}(\text{P}i\text{Pr}_2-\text{NMe}-\text{NH}-\text{P}i\text{Pr}_2)-\kappa^2\text{P,P}']_2(\mu-\text{Cl})_3\}[\text{CoCl}_3(\text{THF})]$ (**11**) exhibits reversible thermochromic behavior in THF solutions and shows no tendency to rearrangement like phosphinohydrazides.

Experimental Session

Solvents were purified following standard methods.¹⁴ Toluene was thoroughly dried and distilled over sodium prior to use. Diethyl ether and THF were dried and distilled over Na/benzophenone. Cobalt silylamide $[\text{Co}\{\text{N}(\text{SiMe}_3)_2\}_2]$ was prepared according to a known method.^{15,16} Methylhydrazine was purchased from Accros Organics Ltd. and was distilled from calcium hydride prior to use. Chlorodiisopropylphosphine, hydrazine dihydrochloride, and 1,2-diphenylhydrazine were purchased from Aldrich Chemical Co. and used as received. All manipulations were performed with rigorous exclusion of oxygen and moisture, in a vacuum or under an argon atmosphere using standard Schlenk techniques. Hexamethyldisilazane liberated in the course of the metal silylamides reactions was detected by gas chromatography analyses with a Tsvet-500 device, equipped with

0.4 cm \times 200 cm stainless steel columns, packed with 5% SE-30 on Chromatone N-Super, with a thermoconductivity detector and with helium as a carrier gas. Spectrophotometric determination of cobalt and nickel in the prepared compounds was carried out by the methods described in ref 17. Infrared spectra were recorded on a Perkin-Elmer 577 spectrometer from 4000 to 400 cm^{-1} in Nujol or on a Perkin-Elmer System 2000 FT-IR spectrometer as KBr mulls. NMR spectra were recorded in CDCl_3 or C_6D_6 solutions using a Bruker DPX-200 spectrometer. EPR spectra were recorded on a Bruker ER 200 D-SRC spectrometer with an ER041 MR microwave bridge, ER 4105 DR double resonator, and ER 4111 VT variable-temperature unit.

X-Ray Crystallography. X-ray data were collected on a Bruker AXS SMART APEX diffractometer for **1**, **5**, **6**, **7**, and **10** and on an Xcalibur-S diffractometer (Oxford Diffraction) for **9**, **11**, and **15** (graphite-monochromator, Mo $\text{K}\alpha$ radiation ($\lambda = 0.71073$ Å), $\varphi-\omega$ scan). All structures were solved by direct methods and were refined on F^2 using SHELXTL¹⁸ and WinGX¹⁹ packages. All non-hydrogen atoms were refined anisotropically. All H atoms in **1**, **5**, **6**, **7**, **9**, and **15** were found from Fourier syntheses of electron density and were refined isotropically. Hydrogen atoms in **10** and **11** (except NH and CH) were placed in calculated positions and were refined in the riding model. SADABS²⁰ and SCALE3 ABSPACK²¹ were used to perform area-detector scaling and absorption corrections. The main crystallographic data and structure refinement details for **1**, **5**, **6**, **7**, **9**, **10**, **11**, and **15** are presented in Table 1.

CCDC - 710335 (**1**), 710336 (**5**), 710337 (**6**), 710338 (**7**), 710339 (**9**), 710340 (**10**), 710341 (**11**), and 710342 (**15**) contain the supplementary crystallographic data for this paper. These data can be obtained free of charge at www.ccdc.cam.ac.uk/const/retrieving.html from the Cambridge Crystallographic Data Centre, 12 Union Road, Cambridge CB2 1EZ, United Kingdom, Fax: (international) +44-1223/336-033, e-mail: deposit@ccdc.cam.ac.uk.

Synthesis. $i\text{Pr}_2\text{P}-\text{NPh}-\text{NPh}-\text{H}$ (1**).** An *n*-hexane solution of *n*-BuLi (1.0 M, 8.2 mL) was added to a stirred solution of 1,2-diphenylhydrazine (1.51 g, 8.2 mmol) in 15 mL of toluene at 0 °C. After stirring for 10 min, $i\text{Pr}_2\text{P}(\text{Cl})$ (1.25 g, 8.2 mmol) in 10 mL of toluene was added dropwise. The colorless solution turned yellow. The reaction mixture was kept at room temperature for 5 h. Lithium chloride was filtered off. Toluene was removed in a vacuum, and diethyl ether (2 mL) was added. Slow crystallization overnight at 0 °C gave colorless crystals of **1**. Yield: 2.09 g (85%). T. subl. 140 °C (0.2 mm Hg). Anal. calcd for $\text{C}_{18}\text{H}_{25}\text{PN}_2$, %: C, 71.97; H, 8.39; P, 10.31. Found, %: C, 71.91; H, 8.42; P, 10.28. ^1H NMR (CDCl_3 , 300 K) δ (ppm): 6.5–7.5 (m, 10H, Ph); 5.8 (s, 1H, NH); 2.0–2.5 (m, 2H, CH), 0.5–1.5 (m, 12H, CH_3). $^{31}\text{P}\{^1\text{H}\}$ NMR (CDCl_3 , 300 K), δ (ppm): 90.2. IR (nujol), $\tilde{\nu}/\text{cm}^{-1}$: 3285m (NH), 1598s, 1307m, 1230s, 1178m, 1154w, 1126m, 1077s, 1025s, 994m, 913, 878, 820, 750vs, 691s, 660m, 640m, 610s, 566s, 511s, 470s.

$i\text{Pr}_2\text{P}-\text{NH}-\text{NH}-\text{P}i\text{Pr}_2$ (2**).** Et_3N (5.56 g, 55.0 mmol) in THF was added to a mixture of hydrazine dihydrochloride (1.05 g, 10.0 mmol) and $i\text{Pr}_2\text{P}(\text{Cl})$ (3.05 g, 20.0 mmol) in THF (20 mL). The mixture was stirred for 24 h at 20 °C and then filtered. The solvent was removed in a vacuum and changed for toluene. Next, the solution was concentrated to ~ 7 mL. Keeping the mixture overnight at 10 °C yielded large colorless crystals of **2**.

(17) Upor, E.; Mohai, M.; Novak, G. *Photometric Methods in Inorganic Trace Analysis*; Academiai Kiado: Budapest, 1985.

(18) Sheldrick, G. M. *SHELXTL* v. 6.12; Bruker AXS: Madison, WI, 2000.

(19) Farrugia, L. G. *J. Appl. Crystallogr.* **1999**, *32*, 837–838.

(20) Sheldrick, G. M. *SADABS* v.2.01; Bruker AXS: Madison, WI, 1998.

(21) *SCALE3 ABSPACK* (Part of the CrysAlis Pro data collection and data reduction software package); Oxford Diffraction Ltd.: Oxfordshire, U.K.

(13) Leal, A. J.; Jimenez Tenorio, M.; Puerta, M. C.; Valerga, P. *Organometallics* **1995**, *14*, 3839–3847.

(14) Perrin, D. D.; Armarego, W. L. F.; Perrin, D. R. *Purification of Laboratory Chemicals*; Pergamon: Oxford, 1980.

(15) Andersen, R. A.; Faegri, K.; Green, J. C.; Haaland, A.; Lappert, M. F.; Leung, W.-P.; Rypdal, K. *Inorg. Chem.* **1988**, *27*, 1782–1786.

(16) Burger, H.; Wannagat, U. *Monatsh. Chem.* **1963**, *94*, 1007.

Yield: 2.43 g (92%). Anal. calcd for $C_{12}H_{30}N_2P_2$, %: C, 54.53; H, 11.44; P, 23.43. Found, %: C, 54.45; H, 11.38; P, 23.60. 1H NMR (C_6D_6 , 300 K) δ (ppm): 3.36 (d, 2H, NH, $^2J_{H,P} = 8.3$ Hz), 1.52–1.78 (m, 4H, CH), 0.9–1.30 (m, 24H, CH_3). $^{31}P\{^1H\}$ NMR (C_6D_6 , 300 K), δ (ppm): 73.6. IR (nujol), $\tilde{\nu}/cm^{-1}$: 3220s, 1630m, br, 1304m, 1260m, 1230s, 1186w, 1152m, 1100m, 1020s, 963w, 924m, 876s, 810s, 655s, 608m, 500m.

***i*Pr₂P–NMe–NH–PiPr₂ (3).** A solution of chlorodiisopropylphosphine (3.05 g, 20 mmol) in THF was added dropwise to a stirred solution of methylhydrazine (1.38 g, 30 mmol) in the same solvent at 20 °C. The mixture was stirred for 3 h and then filtered. The solvent was removed in a vacuum, and pentane was added. Methylhydrazine hydrochloride was filtered off. Pentane was removed in a vacuum, and the residue was distilled at reduced pressure. Bp 100 °C/0.2 mm Hg. Yield: 2.5 g (90%). Anal. calcd for $C_{13}H_{32}N_2P_2$, %: C, 56.09; H, 11.59; P, 22.25. Found, %: C, 55.95; H, 11.52; P, 22.30. 1H NMR (C_6D_6 , 300 K), δ (ppm): 3.37 (s, 1H, NH), 2.78 (s, 3H, MeN), 1.64–1.83 (m, 2H, CH(CH_3)), 1.40–1.56 (m, 2H, CH(CH_3)), 0.70–1.35 (m, 24H, CH_3). $^{31}P\{^1H\}$ NMR (C_6D_6 , 300 K), δ (ppm): 88.9 (s) and 66.5 (s). IR (KBr), $\tilde{\nu}/cm^{-1}$: 3265m (NH), 1188s, 1154m, 1098w, 1017m, 924w, 878m, 809m, 690s, 651m, 603m, 515m.

***i*Pr₂P–NH–NHMe (4).** A solution of chlorodiisopropylphosphine (3.05 g, 20 mmol) in THF was added dropwise to a stirred solution of methylhydrazine (1.84 g, 40 mmol) in the same solvent at 20 °C. The mixture was stirred for 1 h and then filtered. The solvent was removed in a vacuum, and pentane was added. Additional precipitate of methylhydrazine hydrochloride was filtered off. Pentane was removed in a vacuum, and the residue was distilled at reduced pressure. Bp 35 °C (0.2 mm Hg). Yield: 2.9 g (83%). Anal. calcd for $C_7H_{19}N_2P$, %: C, 51.83; H, 11.81; P, 19.09. Found, %: C, 51.79; H, 11.85; P, 19.13. 1H NMR (C_6D_6 , 300 K): δ 3.05 (d, 1H, PNH, $J_{H,P} = 12$ Hz), 2.60 (s, 1H, HNCH₃), 2.32 (s, 3H, NCH₃), 1.60–1.80 (m, 2H, CH(CH_3)), 0.90–1.20 (m, 12H, CH(CH_3)). $^{31}P\{^1H\}$ NMR (C_6D_6 , 300 K), δ (ppm): 65.9 (s). IR (KBr), $\tilde{\nu}/cm^{-1}$: 3267m (NH), 1380m, 1261m, 1231w, 1182m, 1098m, 1019m, 960w, 878s, 807s, 657s, 607w, 517w.

[Li(DME)₃][Li{(NPh–NPh–PiPr₂)– κ N}] (5). Compound **5** was prepared by the addition of an equivalent of *n*-butyllithium to a toluene solution of **1** followed by crystallization from dimethoxyethane. The yield is close to quantitative. Anal. calcd for $C_{48}H_{78}N_4P_2Li_2O_6$, %: C, 65.29; H, 8.90; Li, 1.57. Found, %: C, 65.33; H, 8.94; Li, 1.53. $^{31}P\{^1H\}$ NMR (DME, 300 K), δ (ppm): 83.0 (s).

[Ni{(NPh–NPh–PiPr₂)– κ^2 N,P}] (6). An equivalent of *n*-BuLi in *n*-hexane (5.0 mL, 1 M) was added to a solution of H–NPh–NPh–PiPr₂ (**1**) in THF (1.50 g, 5.0 mmol, 10 mL) at 0 °C. The resulting mixture was kept at 20 °C for 0.5 h and was then added to a suspension of [NiBr₂(THF)₂] (0.91 g, 2.5 mmol) in 10 mL of THF. Nickel bromide dissolved immediately to give a deep blue solution. Keeping the mixture overnight at 0 °C gave a deep blue crystalline precipitate of **6**. Yield: 1.50 g (91%). Anal. calcd for $C_{36}H_{48}N_4P_2Ni$, %: C, 65.77; H, 7.36; Ni, 8.93. Found, %: C, 65.72; H, 7.40; Ni, 8.89. 1H NMR (d^8 -THF, 300 K): δ 6.5–7.4 (m, 20H, Ph), 2.0–2.5 (m, 4H, CH(CH_3)), 1.0–1.4 (m, 24H, CH(CH_3)). $^{31}P\{^1H\}$ NMR (d^8 -THF, 300 K), δ 79.0 ppm. IR (nujol), $\tilde{\nu}/cm^{-1}$: 1590s, 1288m, 1253s, 1225s, 1168m, 1097ww, 1065m, 1029s, 989m, 961s, 890m, 876ww, 8942m, 825m, 752vs, 697s, 669m, 662m, 620m, 546m, 513s. UV/vis spectrum (THF): λ_{max} 350, 530 nm.

[Co{(NPh–NPh–PiPr₂)– κ^2 N,P}] (7). A solution of 1,2-diphenyl-1-(diisopropylphosphino)hydrazine (**1**) in Et₂O (3.00 g, 10.0 mmol) was added to a solution of [Co{N(SiMe₃)₂}]₂ (1.90 g, 5.0 mmol) in the same solvent. The resulting mixture turned dark violet. Dark violet crystals formed rapidly. The mixture was kept at 20 °C for 2 h and then filtered. Crystals of **7** were washed with cold diethyl ether and dried in a vacuum. Yield: 2.80 g (85%). Anal. calcd for $C_{36}H_{48}N_4P_2Co$, %: C,

65.74; H, 7.36; Co, 8.96. Found, %: C, 65.78; H, 7.43; Co, 8.92. IR (nujol), $\tilde{\nu}/cm^{-1}$: 1590s, 1290m, 1230s, 1164m, 1075m, 1021m, 993w, 973m, 879m, 857s, 765m, 754s, 730m, 693s, 669m, 655m, 620m, 573m, 538m, 512m, 501m, 474m. UV/vis spectrum (Et₂O): λ_{max} 420, 538 nm.

[CpNi{(NPh–NPh–PiPr₂)– κ^2 N,P}] (8). A mixture of [Cp₂Ni] (0.19 g, 1.0 mmol) and 1,2-diphenyl-1-(diisopropylphosphino)hydrazine (**1**) (0.30 g, 1.0 mmol) in 15 mL of toluene was heated at 90 °C for 48 h. The green color of the solution slowly turned violet. Toluene was distilled off; the residue was heated in a vacuum at 50 °C to sublime off the unconsumed [Cp₂Ni]. The dark violet product was purified by crystallization from THF to give **8** as fine needles. Yield: 0.27 g (63%). Anal. calcd for $C_{23}H_{29}N_2PNi$, %: C, 65.28; H, 6.91; Ni, 13.87. Found, %: C, 65.31; H, 6.94; Ni, 13.83. 1H NMR (C_6D_6 , 300 K): δ 6.3–7.5 (m, 10H, Ph), 5.3 (5H, s, Cp), 2.0–2.5 (m, 2H, CH), 0.7–1.7 (m, 12H, CH_3). $^{31}P\{^1H\}$ NMR (C_6D_6 , 300 K): δ 67.0 ppm. IR (nujol), $\tilde{\nu}/cm^{-1}$: 1592s, 1288s, 1230m, 1160m, 1074m, 1023m, 960m, 885m, 822m, 780m, 752s, 731w, 693s, 615w, 568w, 512m. UV/vis spectrum (Et₂O): λ_{max} 410, 542 nm.

[FeCl₂{(PiPr₂–NMe–NH–PiPr₂)– κ^2 P,P}] (9). 1-Methyl-1,2-bis(diisopropylphosphino)hydrazine (2.78 g, 10.0 mmol) was mixed with solid anhydrous FeCl₂ (1.27 g, 10.0 mmol). A weak exothermic reaction took place. Toluene (15 mL) was added; the mixture was heated at 80 °C for 20 min. The hot toluene solution was filtered. Slow cooling and keeping the solution at room temperature gave yellow crystals of **9**. Yield: 3.72 g (92%). Anal. calcd for $C_{13}H_{32}N_2P_2FeCl_2$, %: C, 38.54; H, 7.96; Cl, 17.50; Fe, 13.79. Found, %: C, 38.48; H, 8.03; Cl, 17.46; Fe, 13.70. IR (KBr), $\tilde{\nu}/cm^{-1}$: 3240s, 1292w, 1244s, 1214m, 1138s, 1117m, 1023s, 990s, 933m, 882s, 839m, 699s, 667m, 626s, 575m, 489w, 465w, 446w.

[FeBr₂{(PiPr₂–NMe–NH–PiPr₂)– κ^2 P,P}] (10). Complex **10** was prepared and isolated similarly to **9** by reaction of **3** with iron(II) bromide. Yield: 0.66 g (81%). Anal. calcd for $C_{13}H_{32}N_2P_2FeBr_2$, %: C, 31.61; H, 6.53; Br, 32.35; Fe, 11.31. Found, %: C, 31.57; H, 6.58; Br, 32.30; Fe, 11.26. IR (nujol), $\tilde{\nu}/cm^{-1}$: 3250m, 2727w, 1250m, 1215m, 1118s br, 1030m, 993m, 935w, 903w, 882s, 832m, 895s, 670s, 610m, 560m, 472w.

[Co{(PiPr₂–NMe–NH–PiPr₂)– κ^2 P,P}]₂(μ -Cl)₃][CoCl₃(THF)] (11). A solution of 1-methyl-1,2-bis(diisopropylphosphino)hydrazine (**3**) (0.55 g, 2.0 mmol) in THF (5 mL) was added to a solution of CoCl₂ (0.39 g, 3.0 mmol) in the same solvent (25 mL). The mixture turned dark violet-green. Soon, the formation of dark violet crystals was observed. The solution was concentrated to 5 mL; an additional portion of crystals formed. The product was filtered off, washed with cold THF, and dried in vacuum. Yield: 0.90 g (88%). Anal. calcd for $C_{30}H_{72}N_4P_4OCo_3Cl_6$, %: C, 35.38; H, 7.13; Cl, 20.89; Co, 17.36. Found, %: C, 35.32; H, 7.18; Cl, 20.83; Co, 17.31. IR (KBr), $\tilde{\nu}/cm^{-1}$: 3390m, 3216s (ν NH), 1627m (δ NH), 1389m, 1254m, 1221m, 1152m, 1104s, 1033s, 932w, 884s, 729s, 674s, 596m, 549w, 513w, 470w.

Synthesis of LiN=PiPr₂–NMe–PiPr₂ (13) and *i*Pr₂P–NMe–PiPr₂=NH (14) in Situ. An equivalent of *n*-butyllithium (1.0 M solution in *n*-hexane, 2.0 mL) was added to a solution of 1-methyl-1,2-bis(diisopropylphosphino)hydrazine (**3**) (0.56 g, 2.0 mmol) in THF (10 mL). The mixture was kept for 1 h, and then used in further reactions.

An aliquot of the mixture was hydrolyzed by an equivalent amount of a 1 M solution of H₂O in THF. The resulting solution of **14** was studied by $^{31}P\{^1H\}$ NMR δ (ppm): 68.0 (d, $J_{P,P} = 41$ Hz), 59.9 (d, $J_{P,P} = 41$ Hz).

[CoCl₂{(HN=PiPr₂–NMe–PiPr₂)– κ^2 N,P}] (15). A THF solution of **14**, prepared from 0.56 g (2.0 mmol) of **3** as described above, was added to a solution of CoCl₂ (0.26 g, 2.0 mmol) in 15 mL of THF. The mixture was kept for 12 h at

room temperature and then concentrated to 4 mL. Crystallization overnight at 0 °C gave deep blue crystals of **15**. Yield: 0.62 g (76%). Anal. calcd for $C_{13}H_{32}N_2P_2CoCl_2$, %: C, 38.25; H, 7.90; Cl, 17.37; Co, 14.44. Found, %: C, 38.29; H, 7.93; Cl, 17.30; Co, 14.39. IR (KBr), $\tilde{\nu}/\text{cm}^{-1}$: 3264m, 1262s, 1098vs, 1024vs, 929w, 883m, 800vs, 688m, 624w, 498m. UV/vis (THF): λ_{max} 520, 645, 687 nm.

Acknowledgment. This work was supported by The Deutsche Forschungsgemeinschaft (436 RUS 1376/29-1) and

President of RF grant for the support of leading scientific schools (No. 4182.2008.3).

Supporting Information Available: Crystallographic information for **1**, **5**, **6**, **7**, **9**, **10**, **11**, and **15** in CIF format. Molecular structures of **1**, **7**, and **9**; selected bond lengths and angles for **9** and **10**; EPR spectra of **7** and the product of its oxidation; and UV-vis spectra of **11** at various temperatures in PDF format. This material is available free of charge via the Internet at <http://pubs.acs.org>.